

Supporting information for

**Suppress the HSP90-HIF1 α Pathway with a SNX2112
Encapsulated Nano-micelle for Effective Triple-
Negative Breast Cancer Photothermal and
Photodynamic Therapy**

Zhiqi Zhang^{1†}, Fangzheng Tian^{1†}, Shiwei Lai^{1†}, Xiaoxuan Xu¹, Mei Zhou¹, Zhenyu Hou¹, Siyu Li¹, Jianqiong Zhang^{1,2}, Xue Yang¹, Jinbing Xie^{1*}, and Shenghong Ju^{1*}

¹Cultivation and Construction Site of the State Key Laboratory of Intelligent Imaging and Interventional Medicine, Department of Radiology, Zhongda Hospital, Medical School, Southeast University, Nanjing, 210009, China.

²Department of Microbiology and Immunology, Medical School, Southeast University, Nanjing, 210009, China.

[†]These authors contributed equally: Zhiqi Zhang, Fangzheng Tian, Shiwei Lai.

*Correspondence to: jsh@seu.edu.cn (S.J.); xiejb@seu.edu.cn (J.X.)

The PDF file includes:

Fig. S1-S17

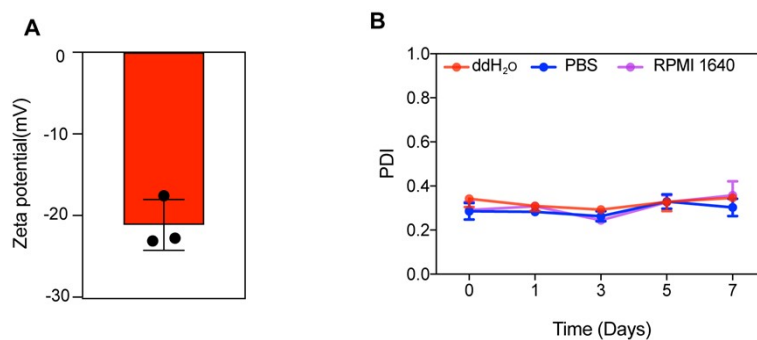


Figure S1. Characterizations of SIDR. (A) Zeta potential of SIDR. (B) Polymer dispersity index (PDI) of SIDR in different environments (ddH₂O, PBS and RPMI 1640) for 7 days.

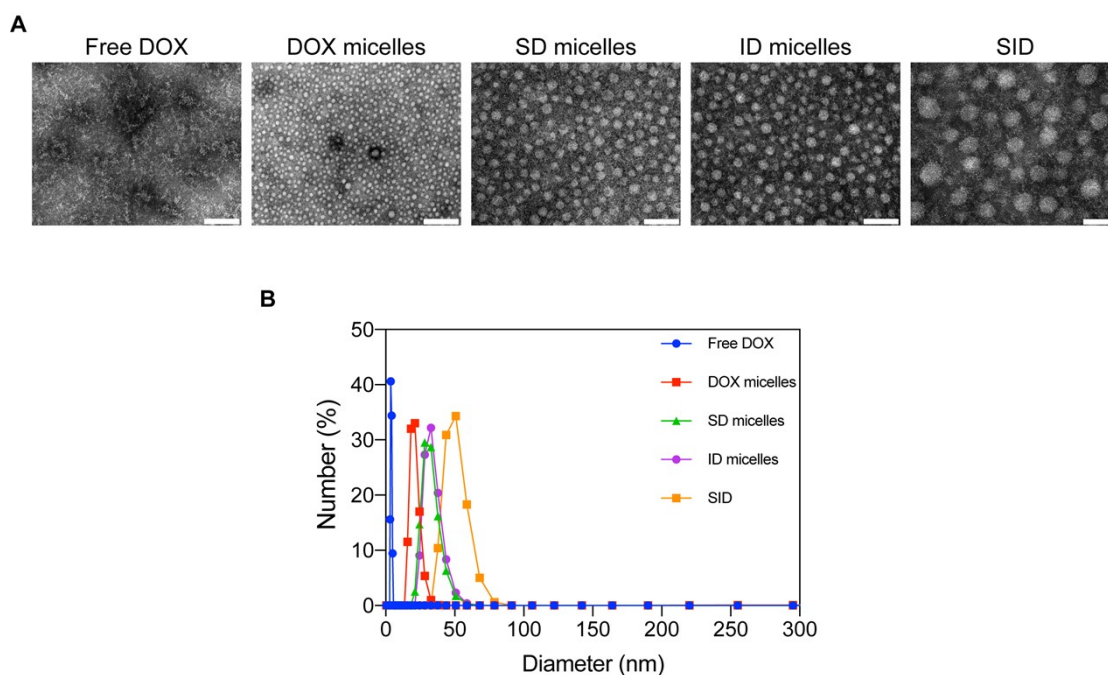


Figure S2. Characterizations of different drug-loaded micelle formulation. (A) the transmission electron microscopy (TEM) images of different drug-loaded micelle formulation (scale bar = 100 nm). (B) Dynamic light scatterings (DLS) analysis of different drug-loaded micelle formulation. DOX micelles (micelles only loaded DOX), SD micelles (micelles loaded SNX2112 and DOX), ID micelles (micelles loaded IR825 and DOX), SID (micelles loaded SNX2112, IR825 and DOX).

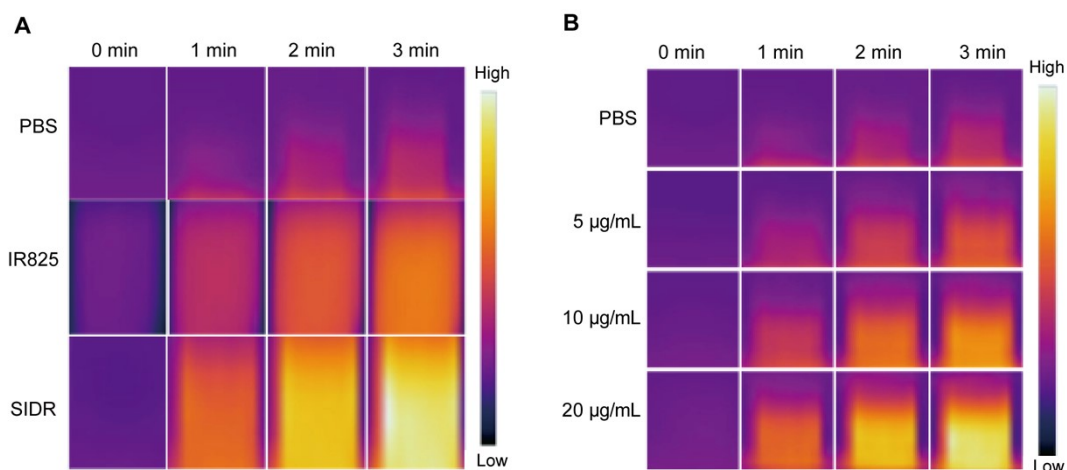


Figure S3. Representative thermal images of SIDR. (A) Representative thermal images of PBS, free IR825 and SIDR in Fig. 1D. (B) Representative thermal images of SIDR with various IR825 concentrations in Fig.1E. All samples were irradiated by laser, 808 nm, 1 W/cm², n = 3.

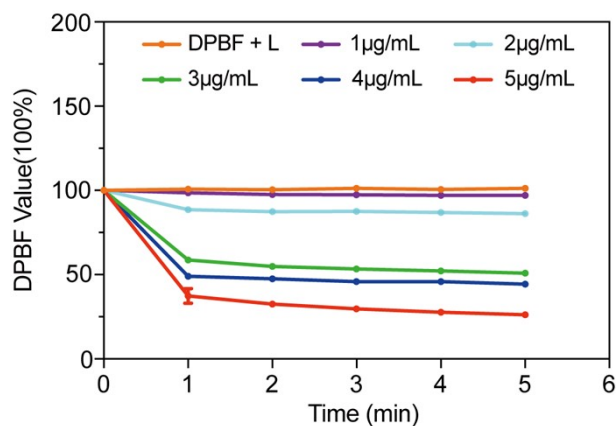


Figure S4. ROS production of SIDR. Relative absorbance of DPBF at 420 nm during ROS detection using DPBF assay of SIDR with various IR825 concentrations. n = 3.

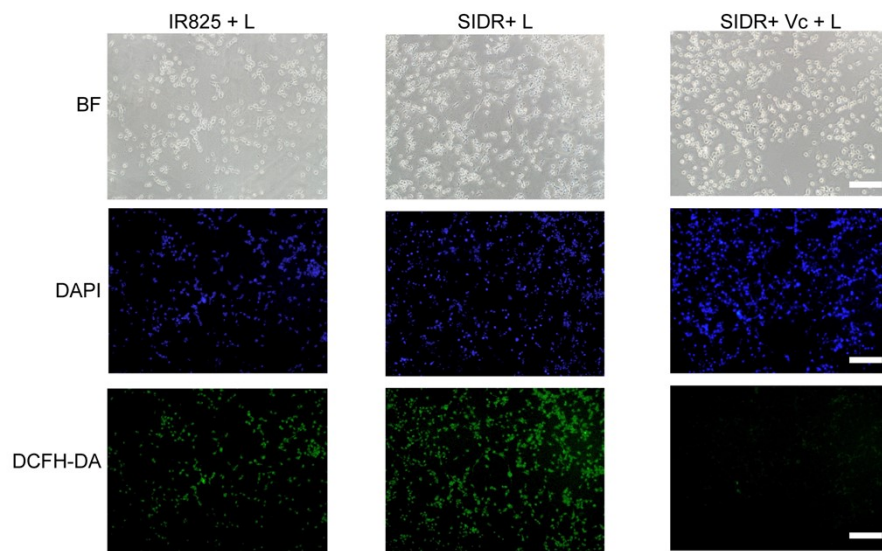
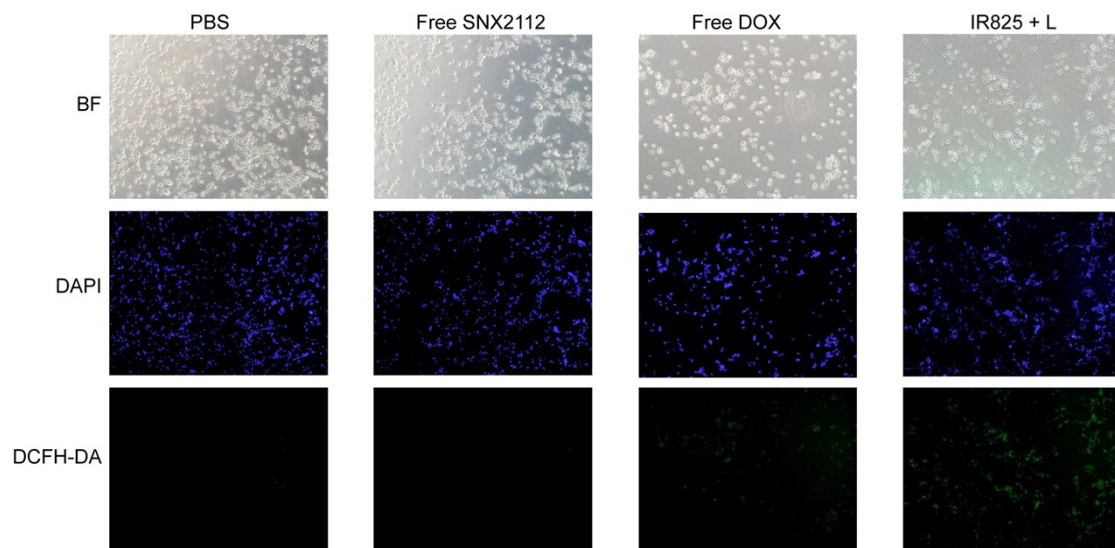


Figure S5. Intracellular ROS detection by DCFH-DA. Representative images of ROS production of SIDR detection by DCFH-DA. Scale bar = 100 μm . L: with laser irradiation, 808 nm, 1 W/cm². BF: bright field.

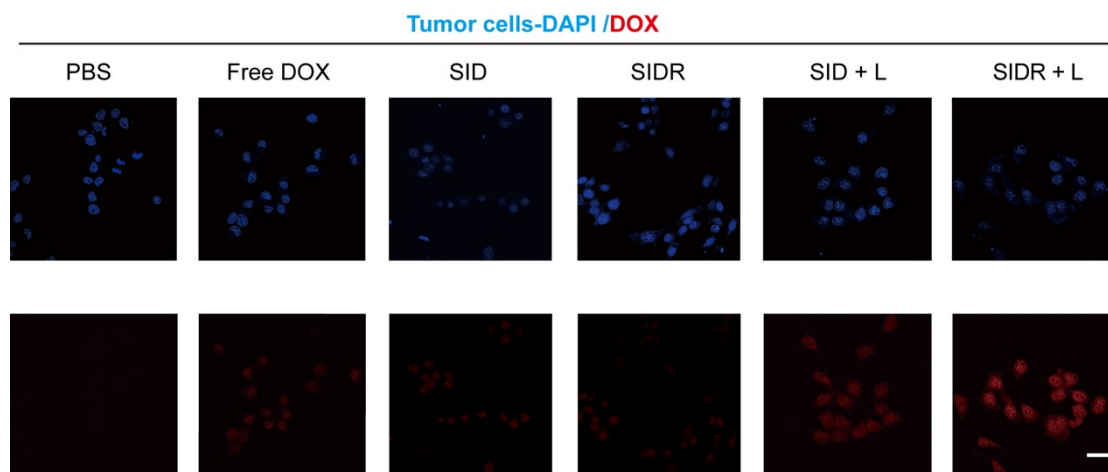


Figure S6. Cell uptake of SIDR in 4T1 cells. Fluorescence images of 4T1 cells incubated with free DOX, SID, SIDR, SID + L and SIDR + L, respectively (scale bar = 30 μm).

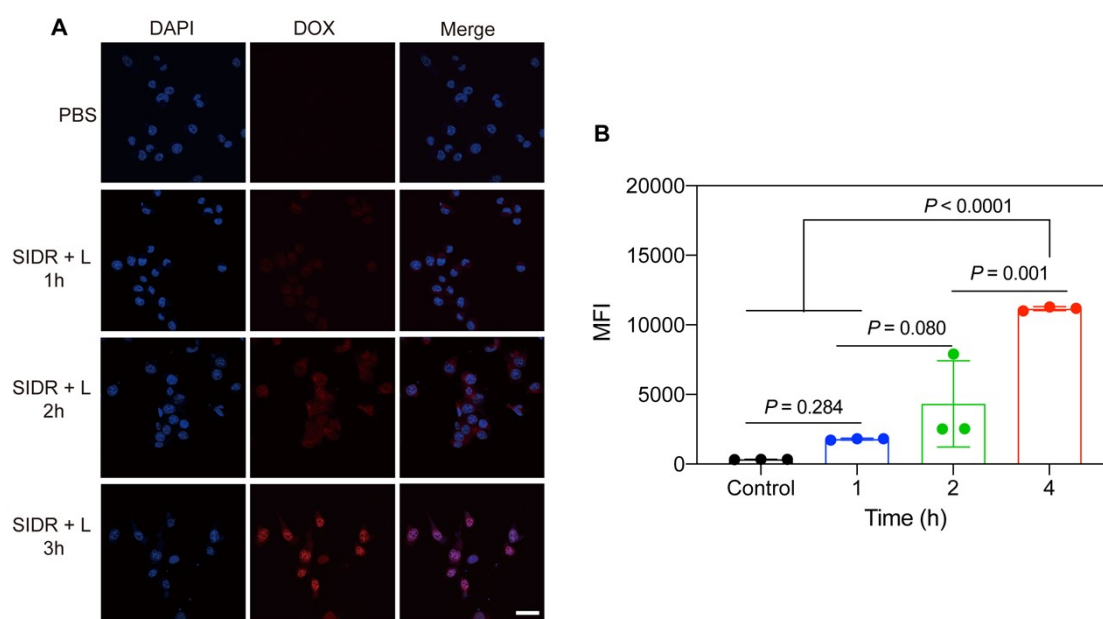


Figure S7. Cell uptake of SIDR in 4T1 cells. (A) Time-dependent fluorescence images of 4T1 cells incubated with SIDR after laser (L: with laser irradiation, 808 nm, 1 W/cm². Scale bar = 30 μm). (B) Quantitative MFI derived from the flow cytometric results in A. Statistical significance was calculated by one-way ANOVA with Fisher's LSD test.

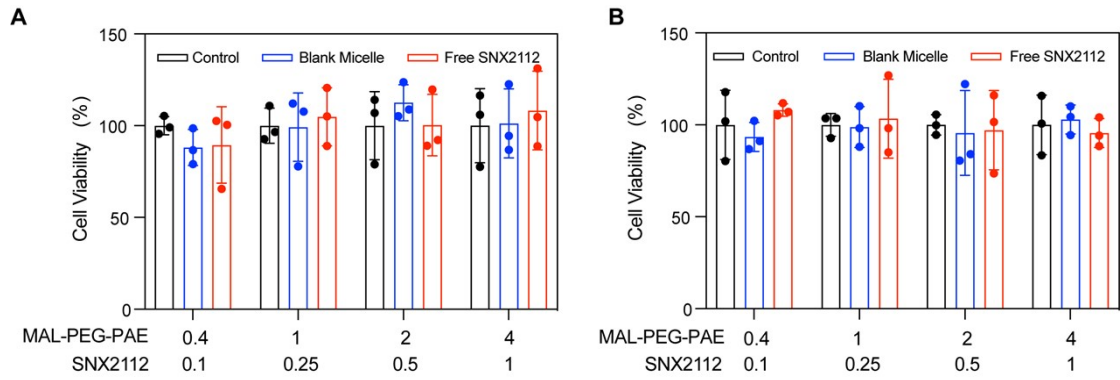


Figure S8. Bio-safety of SIDR in cells. (A) Bio-safety of blank micelle and free SNX2112 in 4T1 cells, $n = 3$. (B) Bio-safety of blank micelle and free SNX2112 in Panc02 cells, $n = 3$, unit: μg , medium volume: $200 \mu\text{L}$.

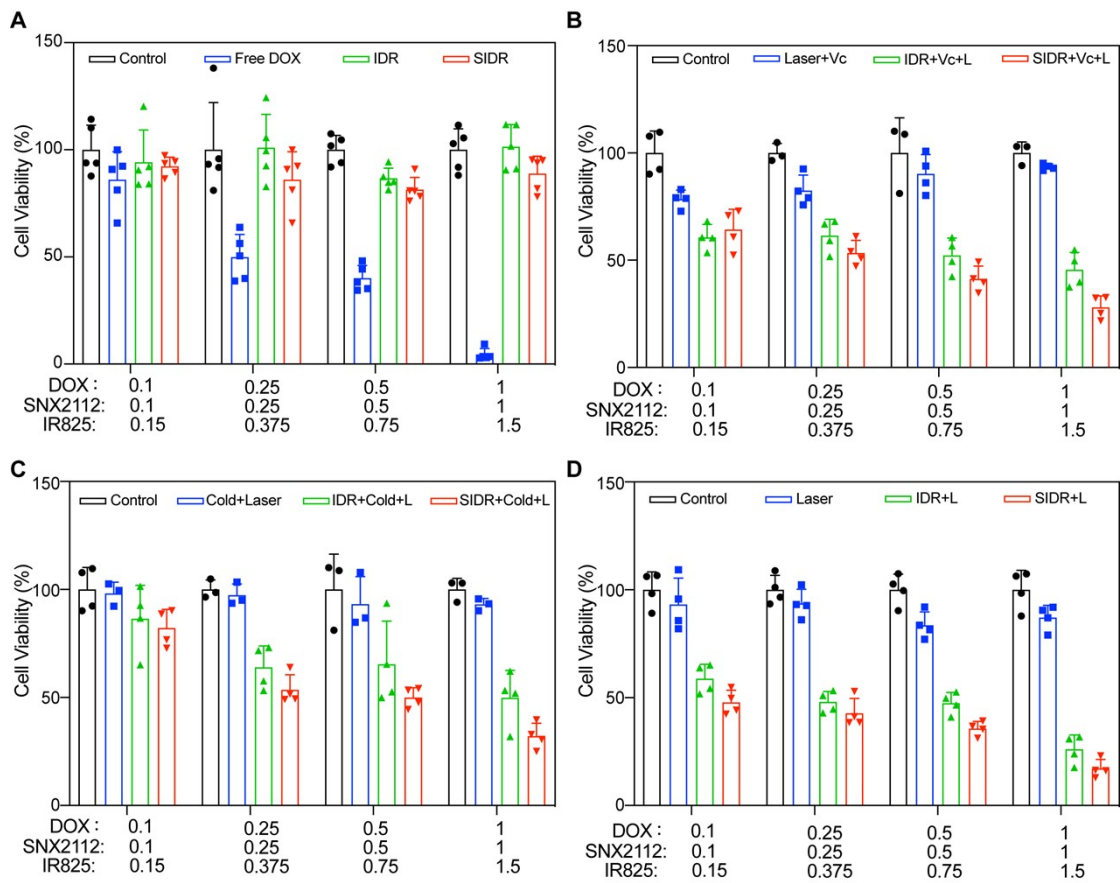


Figure S9. Cytotoxicity of SIDR in Panc02 cells. Relative viability of Panc02 cells with different treatment, which indicate (A) the effect of micelles only, (B) PTT or (C) PDT effect only, and (D) the effect of micelles under irradiation, $n \geq 4$. L: with laser irradiation, 808 nm , 1 W/cm^2 , 3 min , unit: μg , medium volume: $200 \mu\text{L}$.

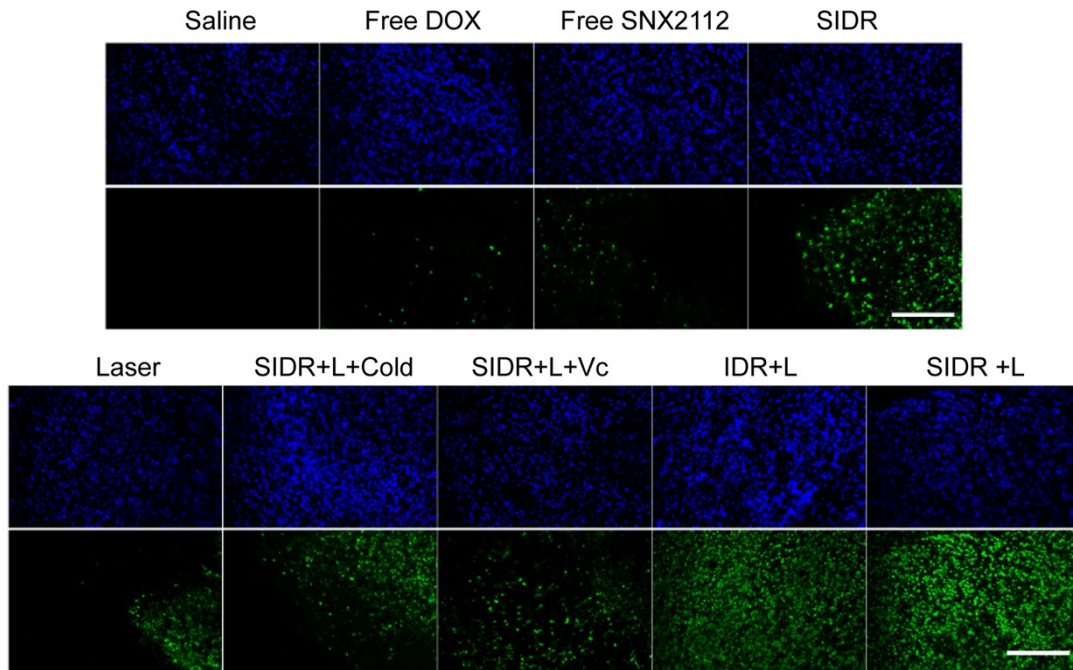


Figure S10. TUNEL staining of 4T1 tumor tissue. TUNEL staining of tumor tissue in different groups of 4T1 tumor-bearing mice after various treatments at day 14. Scale bar = 100 μ m, L: with laser irradiation, 808 nm, 1 W/cm².

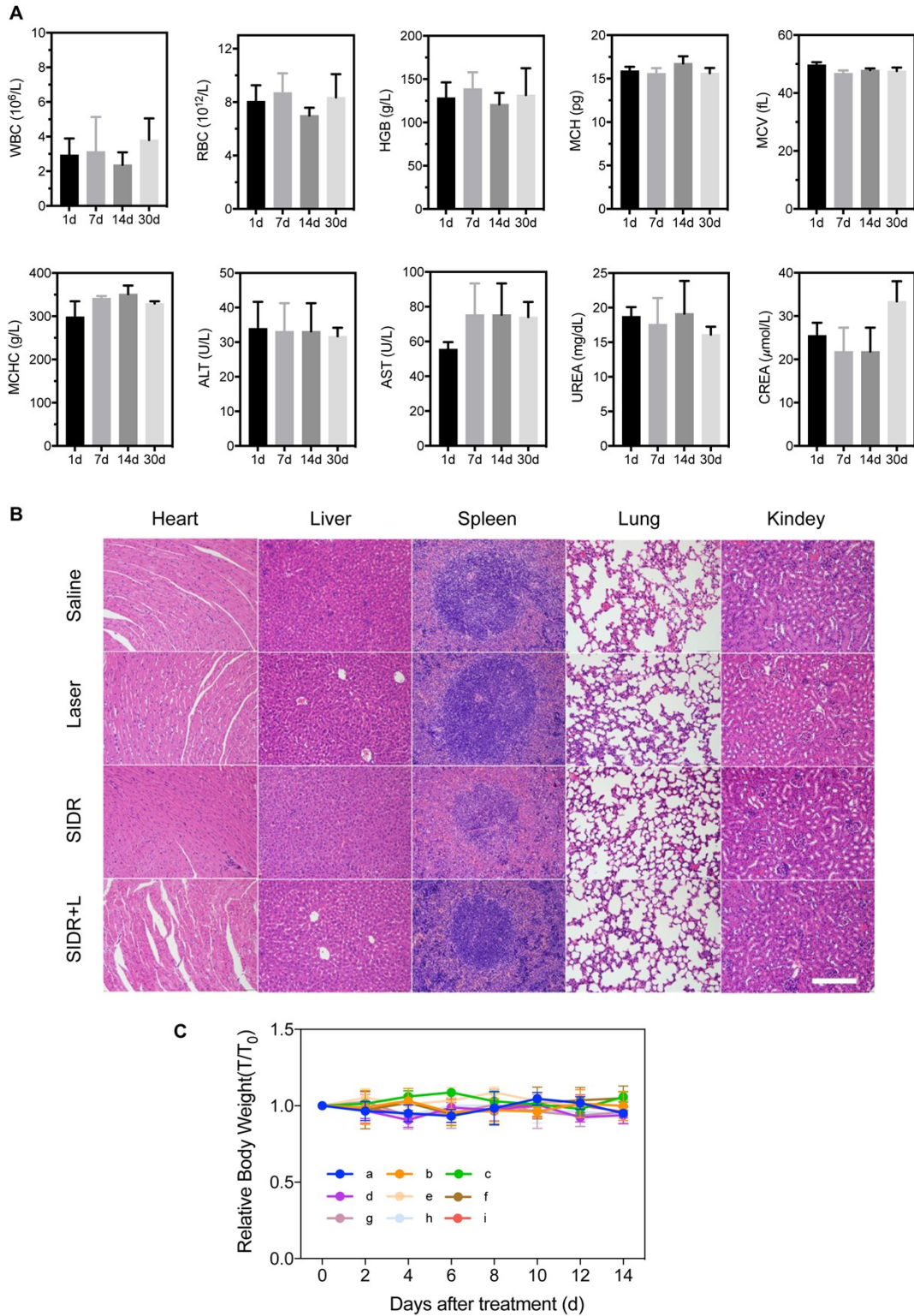


Figure S11. Bio-safety evaluation of SIDR in mice. (A) Hematological indicators of white blood cells (WBC), red blood cells (RBC), hemoglobin (HGB), mean corpuscular hemoglobin (MCH), mean cell volume (MCV), and mean corpuscular hemoglobin concentration (MCHC). Biochemical analysis results of alanine transferase (ALT),

aspartate transferase (AST), urea and creatinine (CREA) 14 days after injections of different treatments. (B) H&E staining of different organs upon treatment 14 days after injections of different treatments. (C) Body weight variation of mice in different groups during a period within 14 days. The groups are (a) Saline (b) Free DOX (c) Free SNX2112 (d) SIDR (e) Laser (f) SIDR + Laser + Cold (g) SIDR + Laser + Vc (h) IDR + Laser (i) SIDR + Laser. L: with laser irradiation, 808 nm, 1 W/cm².

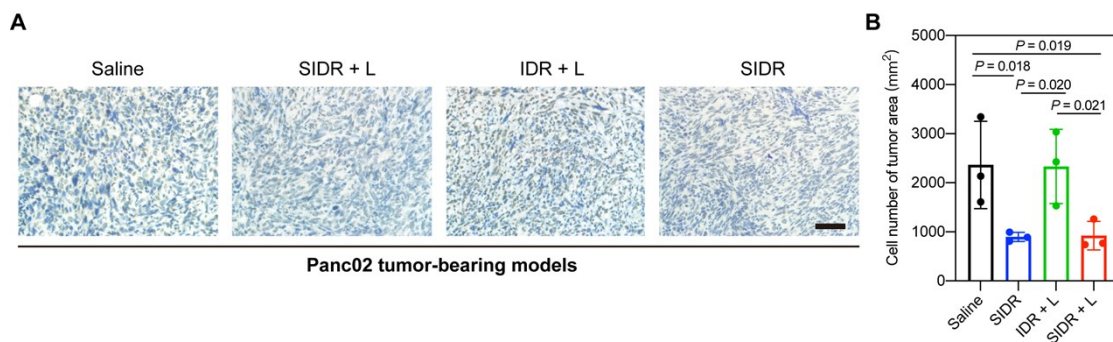


Figure S12. SIDR reduced HIF1 α accumulation in Panc02 tumor-bearing models.

(A) Representative IHC images and (B) qualification of HIF1 α in tumor tissue sections 14 days after injections of different treatments in Panc02 tumor-bearing models, n = 3, scale bar = 100 μ m. Statistical significance was calculated by one-way ANOVA with Fisher's LSD test. L: with laser irradiation, 808 nm, 1 W/cm².

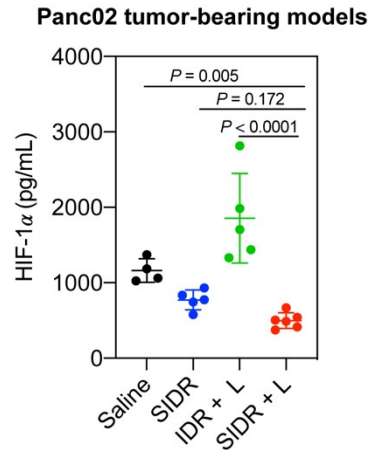


Figure S13. SIDR reduced HIF1 α accumulation in Panc02 tumor-bearing models.

HIF1 α detection by enzyme-linked immunosorbent assay (ELISA) using Panc02 tumor, $n = 5$. Statistical significance was calculated by one-way ANOVA with Fisher's LSD test. L: with laser irradiation, 808 nm, 1 W/cm².

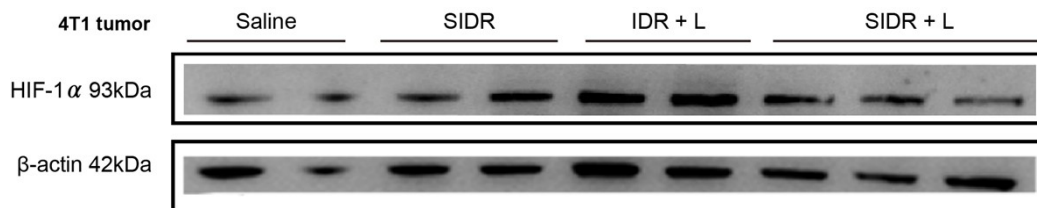


Figure S14. SIDR inhibited HIF1 α expression in 4T1 tumor-bearing models.

HIF1 α detection by WB using 4T1 tumors (14 days after injections of different treatments). 4T1 tumor bearing-mice: Saline and IDR + L treated mice ($n = 4$), SIDR treated mice ($n = 5$), SIDR + L treated mice ($n = 6$). This figure is an addition to the Fig. 5E. L: with laser irradiation, 808 nm, 1 W/cm².

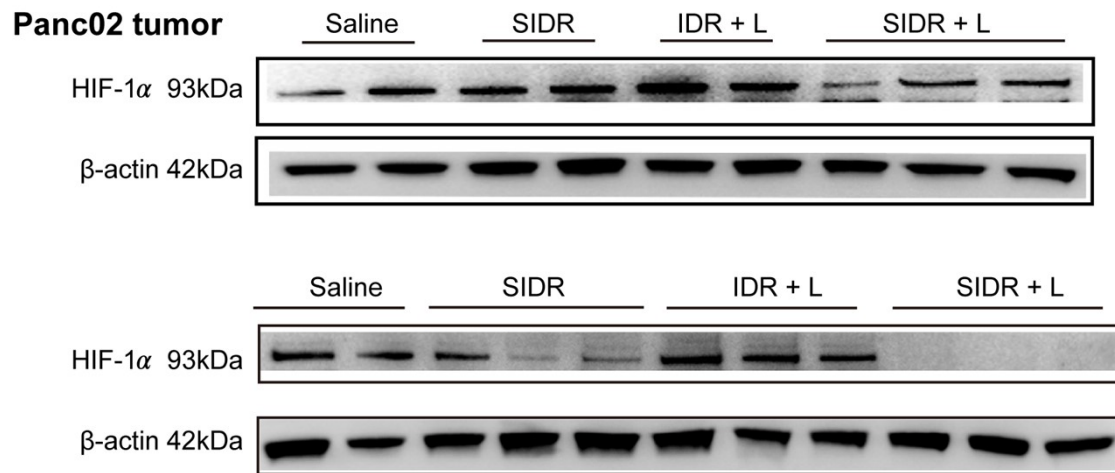


Figure S15. SIDR inhibited HIF1 α expression in Panc02 tumor-bearing models. HIF1 α detection by WB using Panc02 tumors (14 days after injections of different treatments). Panc02 tumor bearing-mice: Saline treated mice (n = 4), SIDR and IDR + L treated mice (n = 5), SIDR + L treated mice (n = 6). L: with laser irradiation, 808 nm, 1 W/cm².

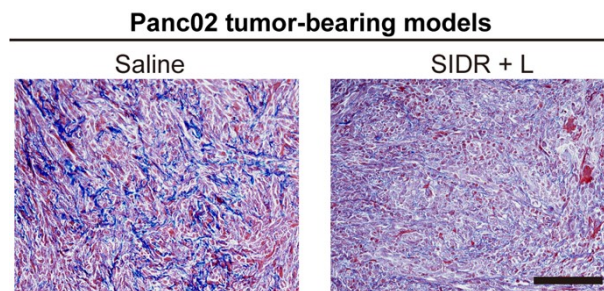


Figure S16. SIDR reduced the fiber barrier in Panc02 tumor-bearing models. Masson staining in tumor tissue sections 14 days after injections of different treatments in Panc02 tumor-bearing models, scale bar = 100 μ m. L: with laser irradiation, 808 nm, 1 W/cm².

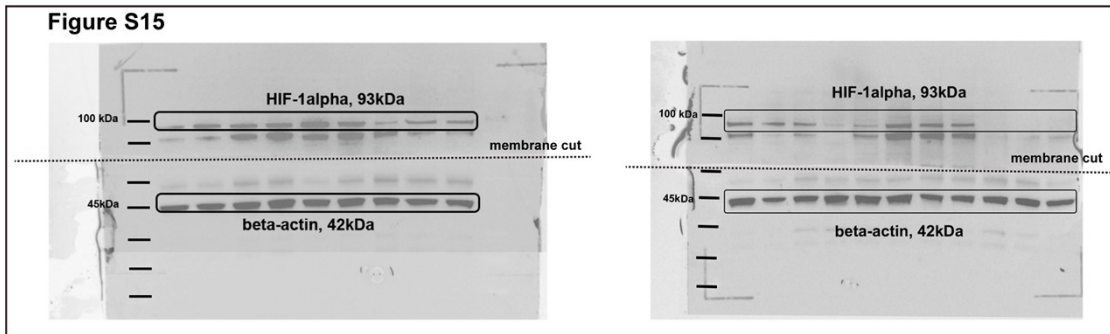
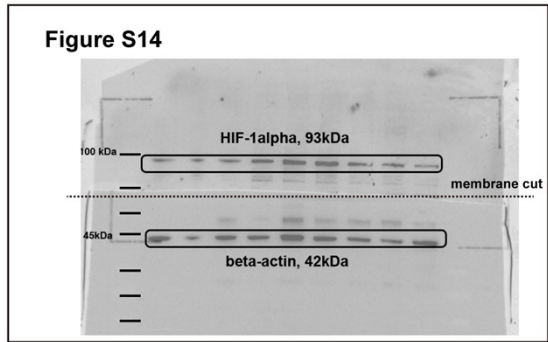
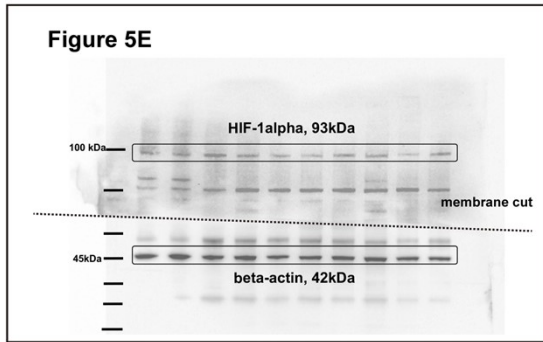
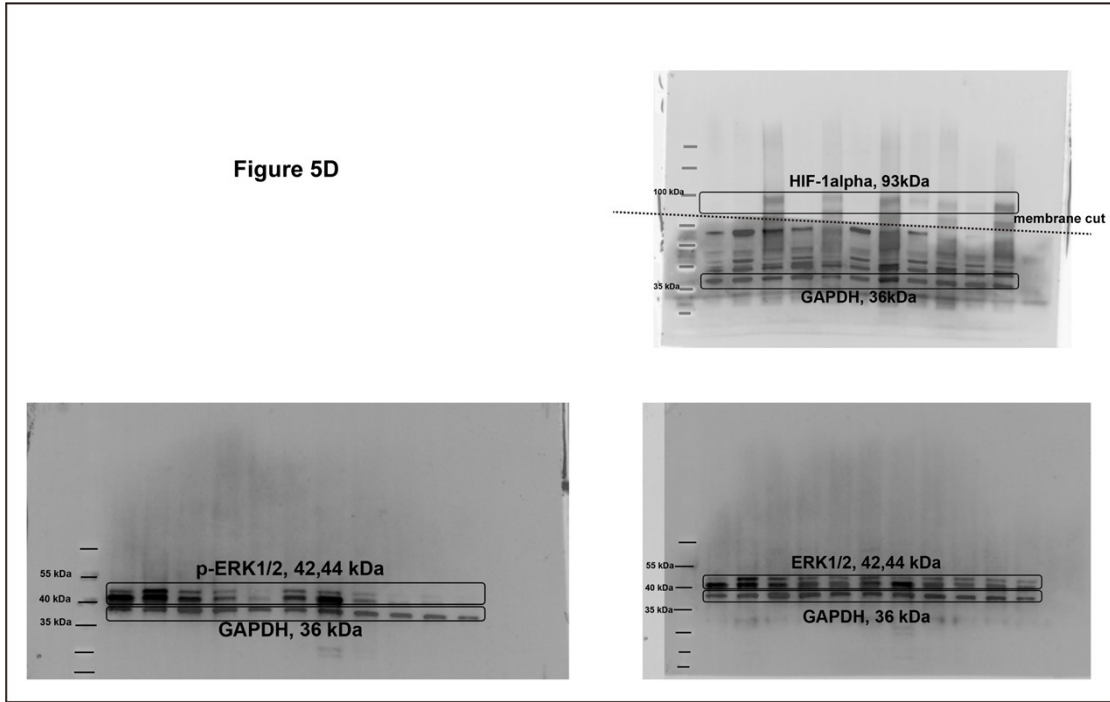


Figure S17. Uncropped Western blot scans.